Silicon (2017) 9:867–877
DOI 10.1007/s12633-017-9568-3

ORIGINAL PAPER

Influence of Thermally Assisted Machining Parameters on the Machinability of Inconel 718 Superalloy

G Venkatesh[1] · D Chakradhar[1]

Received: 25 May 2016 / Accepted: 17 April 2017 / Published online: 25 July 2017

Abstract The present study describes the effect of thermally assisted machining (TAM) parameters on the cutting force, tool wear and surface integrity characteristics (surface roughness, surface topography, and microhardness) of Inconel 718. An inexpensive flame heating technique using oxy-acetylene flame is used to heat the workpiece material. The TAM parameters such as cutting speed, feed rate, depth of cut, and workpiece temperature were selected as process parameters over cutting force, tool wear and surface integrity characteristics.The experimental results reveal that the cutting forces and surface roughness decrease with increases in cutting speed and workpiece temperature, while the workpiece temperature increases as tool wear decreases. The tool wear mechanisms observed were abrasive, adhesive, diffusion and notch wear. The XRD results of thermally assisted machining reveal that neither phase change nor broadening of the peaks were observed at different machining conditions.

Keywords Thermally assisted machining · Cutting forces · Surface roughness · Tool wear · Microhardness · XRD

1 Introduction

Inconel 718 is a nickel - chromium based superalloy, having a significant amount of niobium, chromium, iron, carbon, and molybdenum along with a lesser amount of titanium and aluminum. It exhibits excellent mechanical properties like high strength at elevated temperatures (range of 17–700 °C), high yield and ultimate working temperatures, high corrosion and creep rupture strength and high fatigue endurance limit up to 700 °C, high melting temperatures, and high hot hardness [1–3]. It has good corrosive resistance and high strength with outstanding weldability. The high strength of the material is due to the presence of fine uniform metastable $\gamma'(Ni_3AlTi)$ and $\gamma''(Ni_3AlTiNb)$ intermetallic precipitates distributed throughout the matrix [3]. This superalloy has remarkable advantages in the field of aircraft turbines, nuclear plants, rocket engines, chemical treatment plants, power generation plants, and other challenging environments [4].

Inconel 718 is classified as “difficult to cut” due to its peculiar characteristics such as low thermal conductivity, high tendency to work hardening, presence of abrasive carbide particles, and high affinity for tool materials [5]. For this reason while machining conventionally the problems include excessive tool wear on the cutting tool, a lot of heat generated in the machining zone, built up edge (BUE) formation, increased surface roughness, surface and subsurface defects, such as micro-cracks and surface burn, metallurgical transformation on the surface layer, less metal removal rate, high cutting forces, which results in tensile residual stresses, problems in the deformation and removal of chips, and poor quality of the machined surface which leads to high machining cost [6].

Many researchers and industrial engineers have tried to improve the machinability of difficult to cut materials, using minimum quality lubrication, cryogenic coolants, compressed coolants, new synthetic coolants and hybrid combinations [7]. They reported that better heat control is achieved at the machining zone using various techniques.

✉ G Venkatesh
venkatesh.8056@gmail.com; me12f03@nitk.edu.in

D Chakradhar
chakradhar.d@nitk.edu.in

[1] Department of Mechanical Engineering, National Institute of Technology Karnataka, Surathkal, India

These techniques required coolants to obtain better surface finish and improved tool life. However, these techniques involve high machining cost due to cutting fluid disposal and chip cleaning cost [8, 9].

Thermally assisted machining is an alternative method to improve the tool life, which uses an external heat source to reduce the material strength and hardness. This helps to reduce the cutting forces and makes the material easy to machine [10]. Heat sources vary from primitive to advanced techniques such as induction heating, furnace heating, electric arc heating, electric current heating, flame heating, plasma arc heating and laser beam heating [11]. Due to various reasons some of these methods remain of academic interest only and they are not viable for industrial adoption [7]. In laser assisted machining, the laser beam is focusing on the component, where a narrow beam with high energy softens the workpiece material which facilitates its removal of cutting under low cutting forces compared to conventional machining with increased tool life and greater metal removal rate. However, the laser technique requires high machining cost and large space around the machine tool [12]. The plasma gas technique to heat the workpiece is cheaper compared with laser machining, but it requires high energy consumption besides demanding large space around the machine tool [10].

Compared with various conventional hard turning conditions, TAM is reported to reduce the cutting forces, and give better surface roughness and greater tool life during machining of various materials such as nickel-based superalloys, hardened ferrous alloys, cobalt based alloys and ceramics [12]. Garcia et al. [6] claimed that TAM improved the metal removal rate and tool life while machining Inconel 718 with carbide inserts. Laser heating reduces the chipping and notching of the cutting tool. Kitagawa et al. [13] used plasma as a heat source to machine glasses, ceramics and sintered steel and reported significant improvement in productivity. Hinds et al. [14] suggested an appropriate shape of the heat source, its overall efficiency in this mode and the positioning of the torch. They observed that as the cutting speed increases the efficiency of the heat energy transfer to the workpiece decreases. In TAM of Ti-6Al-4V the cutting forces were reduced by 30%, when the workpiece was preheated to 350 °C. The shortest tool life was observed at 350 °C due to the added heat exacerbating the rate of diffusion wear process. At 150 °C and 250 °C the tool life is increased by 7%. The tool wear mechanisms observed were diffusion wear, adhesive wear and built-up-edge [7]. Attia et al. [15] have used the laser assisted heating technique for machining of Inconel 718 with a ceramic tool (SiAlON) and they found that dominant tool wear mechanisms observed were abrasive and adhesive flank wear. Zhuang et al. [16] have also observed the abrasive wear, adhesive wear, notch wear and flank wear tool wear mechanisms by using preheating and cooling assisted machining of Inconel 718.

Table 1 Chemical composition of Inconel 718

Element	C	Ti	Cr	Fe	Ni	Nb	Mo
Percentage	8.24	0.59	14.81	15.46	54.39	4.10	2.41

The chip form in the TAM and conventional machining was predominantly helical. But the radius of chips curvature produced in the TAM was much larger, tending to the ribbon form. Moreover, the number of lamellas per chip length, i.e., chip formation frequency, in the TAM is greater than in the conventional machining. This indicates a stronger tendency to continuous chip formation and therefore less energy and machining force spent for removing material in TAM [10].

Based on the literature review, limited work has been reported on TAM of Inconel 718. Hence, the present work focuses on thermally assisted machining of Inconel 718 alloy. The main objective of the current study is to investigate the effect of TAM parameters on TAM responses.The TAM parameters considered are cutting speed, feed rate, depth of cut and workpiece temperature. The machinability responses studied are cutting force, tool wear and surface integrity characteristics (surface roughness, surface topography and microhardness).

2 Materials and Methods

2.1 Material selection

Inconel 718 alloy bars of 150 mm length and 35 mm diameter are chosen as the workpiece material and they are heat treated up to 950 °C for one hour, followed by air cooling to relieve residual stresses. The mechanical properties and chemical composition are given in Tables 1 and 2.

2.2 Experimental details

Thermally assisted machining experiments on Inconel 718 were conducted on a Kirloskar lathe machine using a TiAlN

Table 2 Mechanical properties of Inconel 718

Properties	Value
Yield stress (MPa)	1110
Tensile stress (MPa)	1310
Strain (%)	23.3
Elastic modulus (GPa)	206
Thermal conductivity (W/m^2K)	11.2
Density(Kg/m^3)	8470

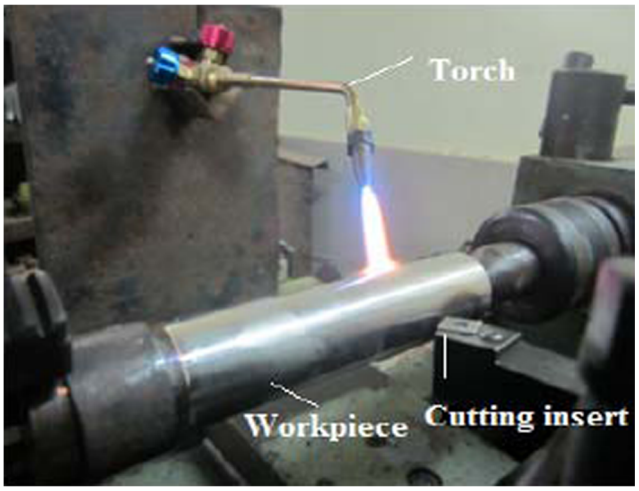

Fig. 1 Experimental set-up of thermally enhanced machining

multilayer coated carbide insert (SNMG120408) with a PSBNR 2020 K12 tool holder. The tool geometry of the insert is inclination angle −6°, rake angle −6°, clearance angle 6°, Major cutting edge angle 75°. The TAM experimental setup is shown in Fig. 1. Cutting inserts used for machining are commercially available and are manufactured by WIDIA of WS10PT grade. The process parameters considered were cutting speed, feed rate, depth of cut and workpiece temperature. The TAM parameters and their feasible ranges are shown in Table 3. In the current study, experiments were conducted based on the one factor at a time approach (OFATA), it is the best design to evaluate the individual performances of the process parameters where the one parameter keeps varying and the remaining parameters were kept constant [17]. Table 4 shows the parameters and their levels used for the current study. We conducted optimization studies for fixing the range of process parameters and constant parameter levels.

Using an electrical furnace, the workpiece is preheated to achieve the desired temperature and thermal equilibrium to enhance the machinability and reduce its shear strength. After the required temperature is achieved, experimental trials were conducted on a lathe machine by fixing the workpiece into the three jaw chuck, the workpiece temperature was measured using a non-contact type high temperature infrared thermometer of model (EQ-8855) wide temperature range of −50 °C to 1050 °C. The temperature of the workpiece loses heat by conduction to steel points of the lathe and heat loss to the atmosphere. To balance the heat loss, oxy-acetylene gas torch heating is utilized. The oxy-acetylene torch was attached to opposite sides of the tool carriage to maintain the temperature of the workpiece properly as shown in Fig. 1. After the required temperature is achieved cutting trails were performed, ±15 °C is acceptable as the temperature tolerance for experiments. For each experiment, TAM is performed with constant machining time of 4 minutes. An IECIOS dynamometer of model 620 series mounted on the tool post of the machine along with a three channel amplifier model 652 with computer interface is used for on-line measurement of the cutting forces. After each trial, optical and scanning electron microscopy was used to measure the tool flank wear. The surface roughness of the machined samples was measured using a Mitutoyo surface tester SJ301. For each cutting trail the average of three sampling measurements was taken with a cutoff length of 0.8 mm and a stylus speed of 0.25 mm/s. The surface topography was measured with a "LEXT OLS400" laser microscope. Laser scanning was used to measure the surface profiles of the TAM machined components. In the machined samples, a scanning area of 120 × 120 μm and 2592 X magnification was employed for measuring the surface topography. To study the surface topography on the machined surface the workpiece is cut into small specimens of size 10 mm × 10 mm × 10 mm by a wire electro-discharge machine. The microhardness of the cross-section of the TAM machined surface was measured on an OMNI TECH MVH-S-AUTO. The cross-section samples were polished by SiC papers of different grades to remove the scratches present on the surface and a diamond polish is used to get the mirror finish on the specimen.

Table 4 Constant process parameters during thermally assisted machining

Control parameters	Level
Cutting speed (m/min)	90
Feed rate (mm/rev)	0.048
Depth of cut (mm)	0.6
Workpiece temperature (°C)	600

Table 3 Thermally assisted machining process parameters and their levels

Symbol	Control parameters	Level – I	Level – II	Level – III	Level – IV	Level – V
v	Cutting speed (m/min)	18	34	52	72	90
f	Feed rate (mm/rev)	0.048	0.071	0.096	0.119	0.143
d	Depth of cut (mm)	0.2	0.3	0.4	0.5	0.6
T	Workpiece temperature (°C)	200	300	400	500	600

Marble's reagent 10g $CuSO_4$+ 20ml HNO_3+ a few drops of H_2O was used to etch the specimen of Inconel 718. The etching time of the polished specimen was 10 seconds. X-ray diffraction was measured with a "JOEL, JDX-P" machine. The XRD was measured on the machined surface.

3 Results and Discussion

3.1 Analysis of cutting force

Figure 2 shows the effect of thermally assisted machining process parameters on cutting forces. Figure 2a shows the influence of cutting speed on cutting force with constant parameters of feed rate 0.048 mm/rev, depth of cut 0.6 mm, and workpiece temperature 600 °C. It was observed that as cutting speed increases from 18 m/min to 90 m/min the cutting force decreases drastically by 47.66%. This effect is mainly due to the high temperature developed at higher cutting speeds which in turn increase the shear plane angle leading to softening of the workpiece, and reduction of chip thickness resulting in lower cutting force [18]. From Fig. 2b as the given values of feed rate increase the cutting force increases linearly by 101.66%, due to increase in feed rate contact area between tool tip and workpiece which in turn increases the plastic deformation, resulting in decreasing the cutting force. At lower feed rate the resistance to tool in the direction of feed rate is much less, on the other hand, as the feed rate increases the workpiece material offers high resistance in the direction of the cutting tool, which

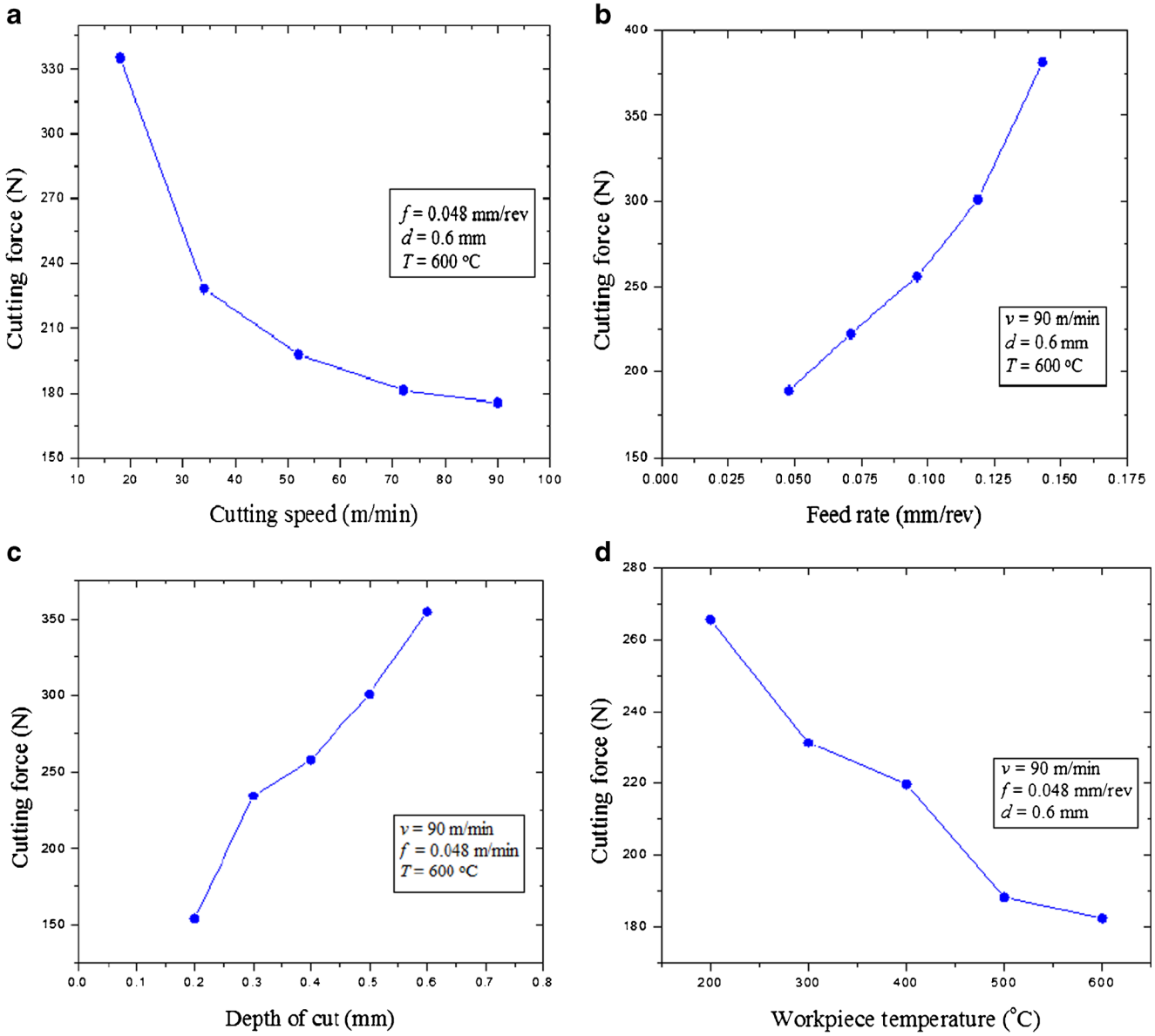

Fig. 2 Effect of TAM parameters on cutting forces

leads to increase in cutting force. As shown in Fig. 2c with increase in the depth of cut, the cutting forces increases by 130.30%. From Fig. 2d it is observed that as workpiece temperature increases cutting force decreases by 31.36%. This significant effect is mainly due to the reduction of yield strength of the machining workpiece resulting in less cutting force generation.

3.2 Analysis of Surface roughness

The surface roughness of thermally assisted machining of Inconel 718 mainly depends on the machining conditions and mechanical properties. Figure 3a depicts the effect of cutting speed on surface roughness with constant parameters of feed rate 0.048 mm/rev, depth of cut 0.4 mm and workpiece temperature 600 °C and variation of surface roughness against cutting speed. It is observed that with the increase in cutting speed from 18 to 90 m/min, the surface roughness is sharply decreased from 1.37 μm to 0.41 μm which is 72.99%. The probable reason might be that as the cutting speed increases the heat generation at the cutting zone increases, leading to thermally softening of the workpiece material and thus reducing the surface finish. Figure 3b shows the variation of surface roughness against feed rate. As the feed rate increases the surface roughness value also increases by 266.66%. This is because with increased feed rate, the thrust force increases leading to generating more heat and vibration thereby resulting in higher surface roughness [19]. Figure 3c shows that on increasing surface roughness by 141.17% a trend was observed due to

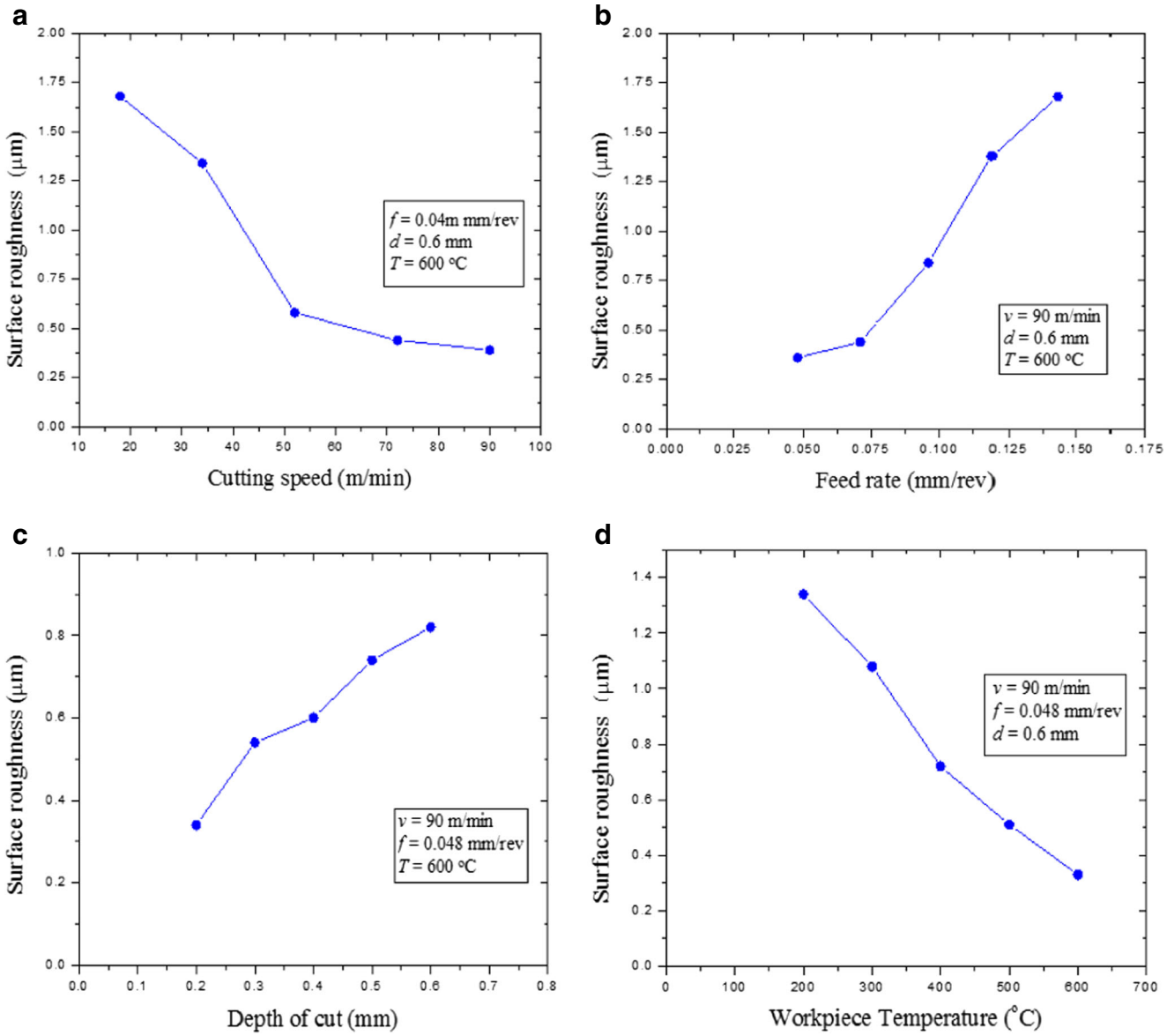

Fig. 3 Effect of TAM parameters on surface roughness

restructuring of surface flaws and discontinuities with increase in depth of cut. As seen from Fig. 3d as the workpiece temperature increases the surface roughness decreases by 75.37% and can be attributed to these three mechanisms: (i) reduction in cutting forces indirectly reducing the chatter vibration [11], (ii) continuous chip formation instead of discontinuous chip formation, (iii) reduction in the tendency to form a built up edge.

3.3 Analysis of tool wear

Flank wear is most generally used to estimate the tool condition. It normally occurs on the relief face or flank of the tool cutting edge Flank wear occurs due to the presence of abrasive particles present in the workpiece material. The tool wear on Inconel 718 superalloy of thermally assisted machining mainly depends on the process parameters. Figure 4a depicts the effect of cutting speed on flank wear with constant parameters of feed rate 0.048 mm/rev depth of cut 0.6 mm and workpiece temperature 600 °C. The tool flank wear is increased with the increase in cutting speed by 166.66% Flank wear is observed to be higher at higher cutting speeds. With the increase in cutting speed, the rubbing action between the tool and the workpiece is faster and high cutting temperatures are generated even though there is less contact time. This effective absorption of high cutting temperatures generates close to the cutting edge. From this cutting condition, the strength of the cutting tool is reduced

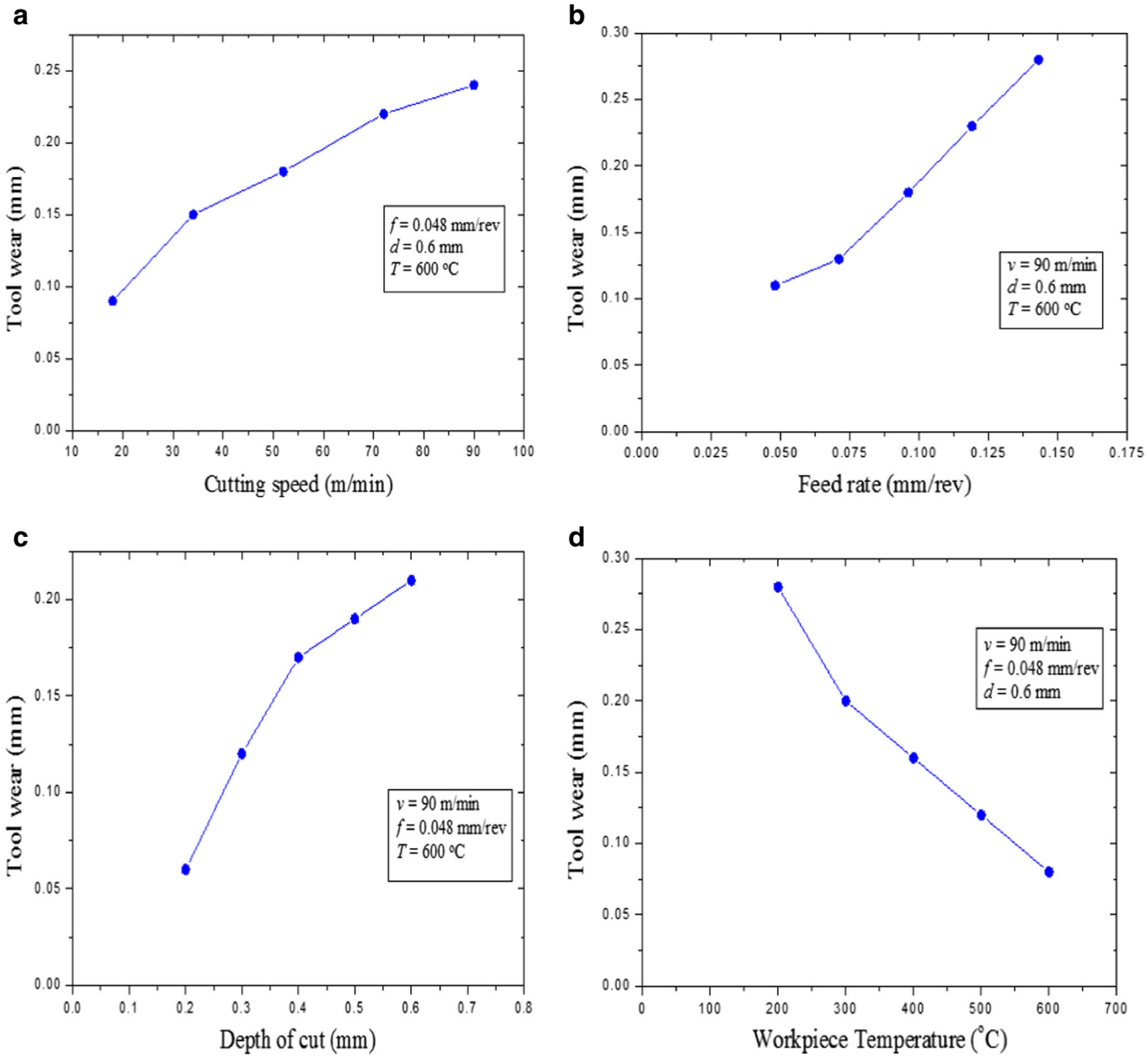

Fig. 4 Effect of TAM parameters on tool wear

with the rubbing action over the surface. Figure 4b and c illustrate that as feed rate and depth of cut increases the flank wear also increases by 154.54% and 250%, the reason being the increase in cutting forces which weakens the cutting tool. High cutting temperatures and high stresses generated at the rake and flank face close to the nose area probably cause the yield strength of the tool to reduce flank wear. Figure 4d shows that as workpiece temperature increases from 200 °C to 600 °C the flank wear decreases by 67.85%. This may be due to the fact that flank wear decreases which is mostly due to reduction of shear strength of the workpiece material due to heating causing less friction at the tool-chip interface causing a significant decrease in flank wear.

3.4 Tool wear mechanisms

During thermally assisted machining of Inconel 718, there are different types of wear observed, namely abrasive wear, adhesive wear, chemical wear and diffusion wear.

Figure 5 shows SEM micrographs of cutting tools after TAM operation at different cutting parameters. Experiments were performed at low and high levels of each process parameter and the remaining parameters kept constant as shown in Table 4. In this study at low cutting speed 18 m/min the tool surface was very smooth and much less amount of wear debris was observed on the tool surface. The tool wear mechanism observed was mainly abrasive

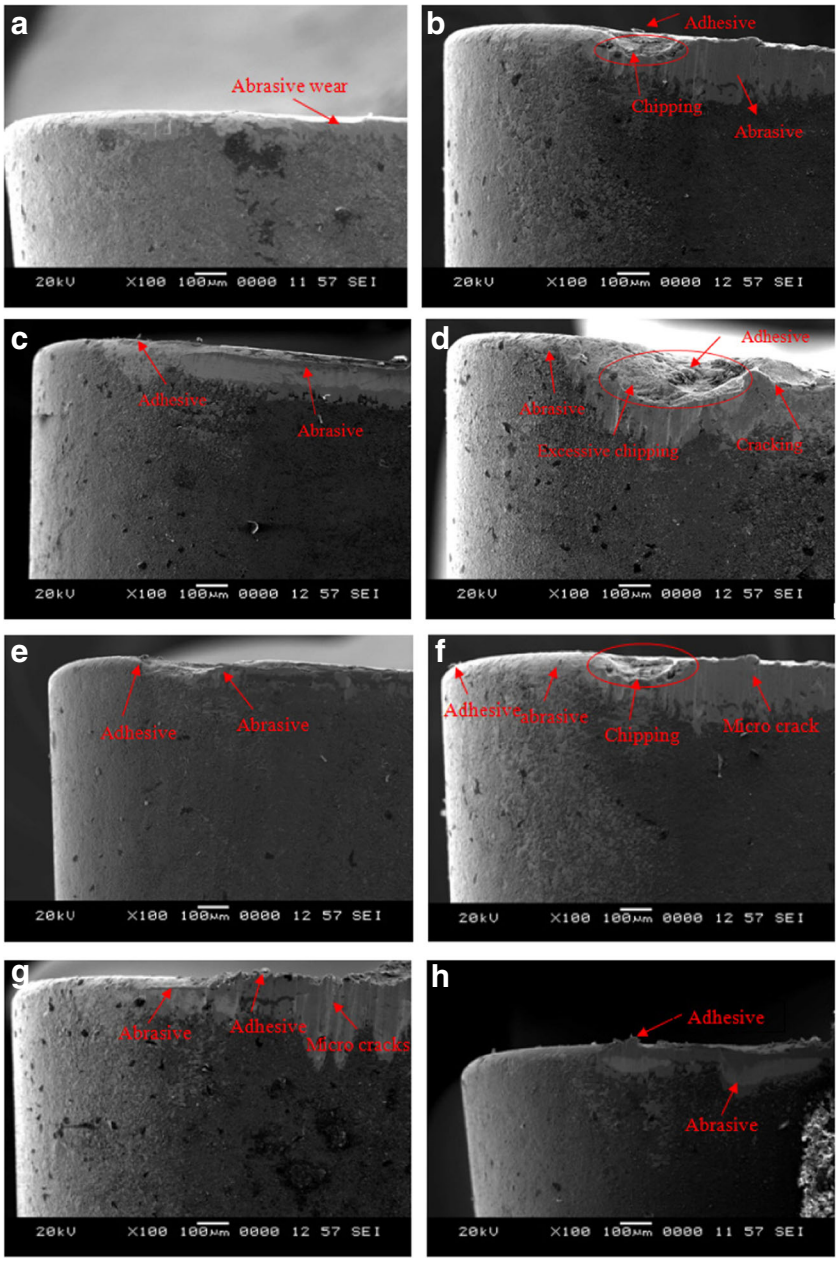

Fig. 5 SEM images of tool flank wear at **a**) cutting speed at 18 m/min **b**) cutting speed at 90 m/min **c**) feed rate at 0.048 mm/rev **d**) feed rate at 0.143 m/min **e**) depth of cut at 0.2 mm **f**) depth of cut at 0.6 mm **g**) workpiece temperature at 200 °C **h**) workpiece temperature at 600 °C

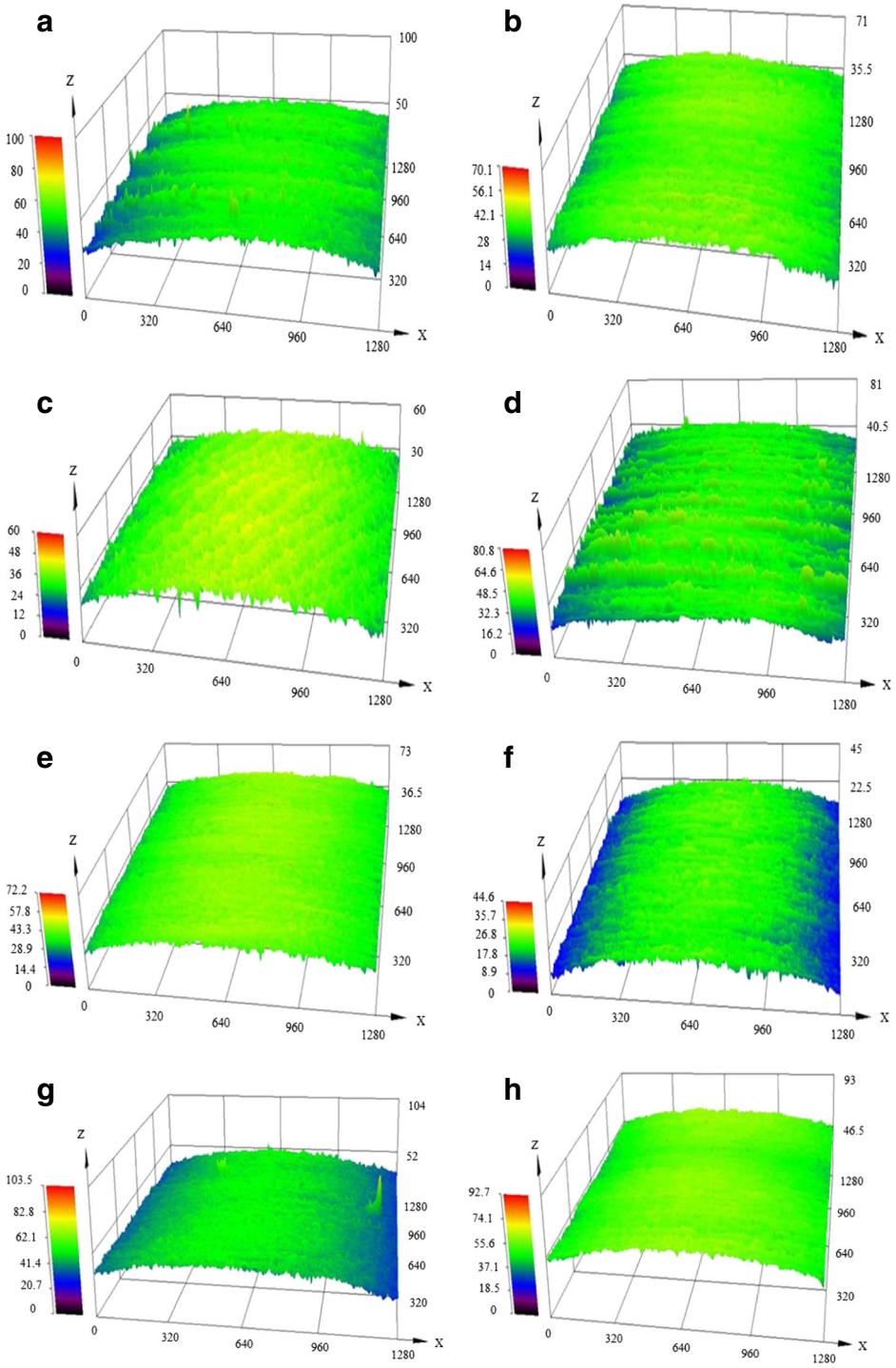

Fig. 6 Surface topography of TAM surface **a**) cutting speed at 18 m/min **b**) cutting speed at 90 m/min **c**) feed rate at 0.048 mm/rev **d**) feed rate at 0.143 m/min **e**) depth of cut at 0.2 mm **f**) depth of cut at 0.6mm **g**) workpiece temperature at 200 °C **h**) workpiece temperature at 600 °C

wear. Due to the presence of hard abrasive, carbide particles present in the workpiece material and plucked off particles from the tool substrate are responsible for abrasive wear [20] as shown in Fig. 5a. Further at higher cutting speed 90 m/min abrasive wear, adhesive wear and chipping of the flank wear were observed in Fig. 5b. On the other hand at low feed rate 0.048 mm/rev, the tool wear is low because the contact area between tool and workpiece is much less and also the temperature is not so high to plastically deform the workpiece material at low level causing adhesion as shown in Fig. 5c. At high feed rates 0.143 mm/rev, abrasive, adhesive wear and excessive chipping were observed. The adhesive wear is due to the high temperatures generated at the tool work interface which leads to welding occuring

between chip and tool. Frequent formation and diminishing of adhered particles lead to fluctuation of cutting forces causing excessive chipping on the tool surface. It also causes cracking between tool coating and tool substrate and then the PVD coating is cut by the workpiece and peels off as the cutting process continues, as shown in Fig. 5d.

According to Fig. 5e and f depth of cut has less effect on tool wear. In low depth of cut 0.2 mm the tool wear mechanism observed was abrasive and adhesive wear. In higher depth of cut 0.6 mm the tool flank wear increases due to contact between the tool and workpiece increasing. From Fig. 5g at low workpiece temperature 200 °C the tool flank wear increases due to the adhesive layer built up edge formation on the tool surface. This layer is formed due to the high temperatures generated at the tool and the workpiece during machining. Also, at high temperature, the transfer of elements between tool and workpiece penetrates to the tool causing diffusion wear and thermal fatigue cracks [17]. It is observed that in Fig. 5h at a high workpiece temperature 600 °C the flank wear was much less. This effect is due to heating of the workpiece causing reduction of shear strength at the cutting zone leading to reduction of cutting forces and flank wear. The other reason might be that due to heating the workpiece becomes soft and friction between tool and chip reduces, the reduction of thrust force leads to reduced flank wear. Similar discussions were found elsewhere [2, 12].

3.5 Surface Topography

The surface topography of thermally assisted machining of Inconel 718 machined surface is shown in Fig. 6. Experiments were performed at low and high levels of each process parameter and the remaining parameters kept constant as shown in Table 4. Figure 6a shows that at low cutting speed 18 m/min the intensity of the peaks is high, larger and deeper craters on the machined sample lead to poor surface finish. Better smoothness and fine surface can be obtained at higher cutting speeds 90 m/min, because as the speed increases the cutting temperature increases at the cutting zone causing thermal softening of the material and less surface roughness. According to Fig. 6b it is evident that the intensity of the peaks is less on the machined surface at high cutting speeds 90 m/min, hence good surfaces were observed. Then by comparing the average surface roughness of the machined workpiece at cutting speed of 18 m/min and 90 m/min the difference of 0.96 μm is found which indicates that cutting speed has a significant effect on average surface roughness. Similarly, by comparing the average surface roughness of the machined workpiece at a feed rate of 0.048 mm/rev and 0.143 mm/rev, the difference of 1.17 μm shows that feed rate has another great influence affecting surface quality of the machined workpiece as shown in Fig. 6c and d.

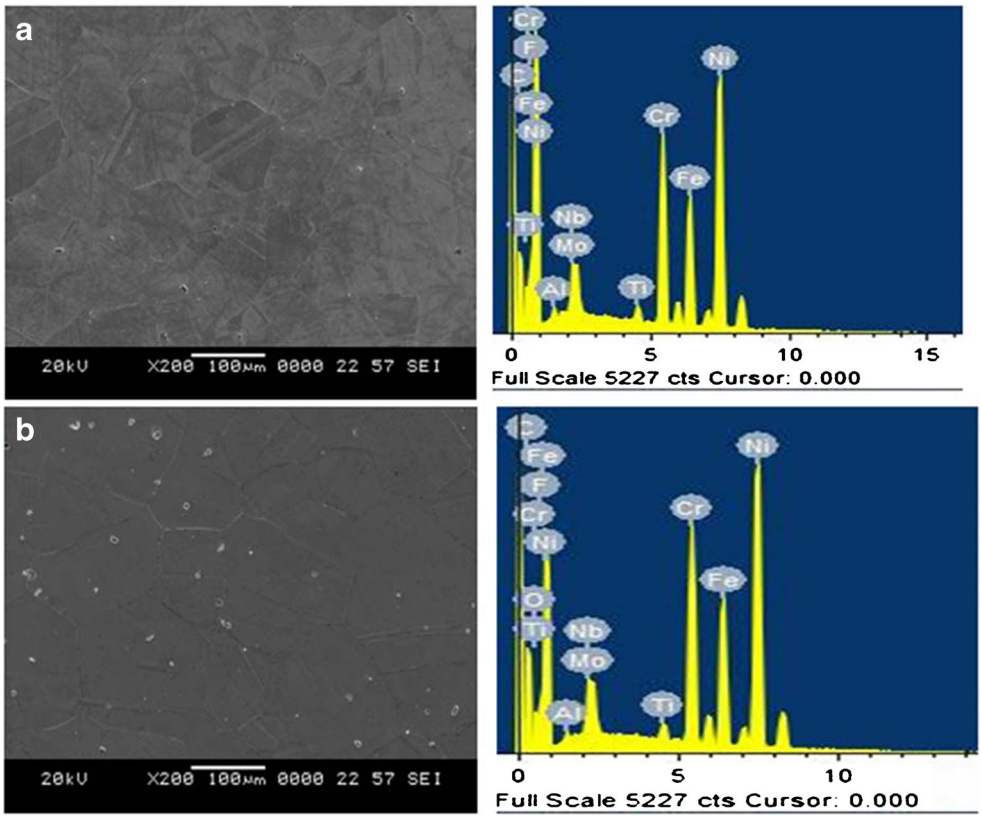

Fig. 7 Microstructure and X-ray spectroscopy obtained at **a**) Room temperature **b**) Thermally assisted machining

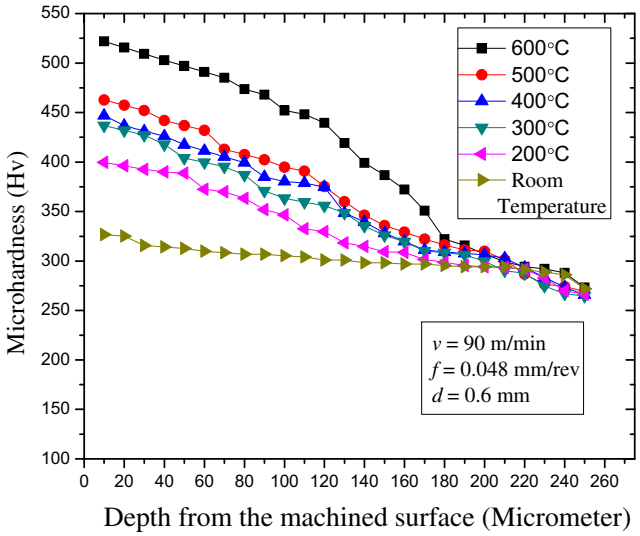

Fig. 8 Subsurface hardness profiles of thermally assisted machined components

Figure 6e shows the smooth surface of the machined surface at low depth of cut 0.2 mm because contact between tool and workpiece is much less. But at higher depth of cut 0.6 mm the surface roughness increases due to restructuring of surface flaws and discontinuities are observed as shown in Fig. 6f. From Fig. 6e and f it is evident that the depth of cut has negligible effect on surface roughness. From Fig. 6g it is observed that at low workpiece temperature 200 °C the surface roughness is increasing because of cutting forces and chatter vibrations. On the other hand at high workpiece temperature 600 °C the smoother and better surface roughness is observed as shown in Fig. 6h. Because high temperature softening of the material affects low cutting forces, the mechanism of chip changes from discontinuous to continuous leading to smoother surface roughness.

3.6 Microstructure

Figure 7a and b shows the microstructure and X-ray spectroscopy of the material before and after thermally assisted machining respectively. X-ray spectroscopy shows that there is no significant change in TAM compared to the bulk material, it also indicates that there is no phase transformation taking place in the machined surface.

3.7 Microhardness

The microhardness of the machined samples of Inconel 718 by thermally assisted machining was measured at different workpiece temperatures 200, 300, 400, 500 and 600 °C keeping other parameters constant as shown in Fig. 8. The nearby portion of the machined surface was considered as a reference point (0 μm) because it is very hard to measure the microhardness precisely on the machined surface due to improper indentation. Microhardness of TAM of Inconel 718 was observed to be high in the near surface layer, and then it was found to decrease rapidly. As the workpiece temperature increases the microhardness value increases.The probable reason might be, as the temperature increases grain refinement occurs on the machined surface,

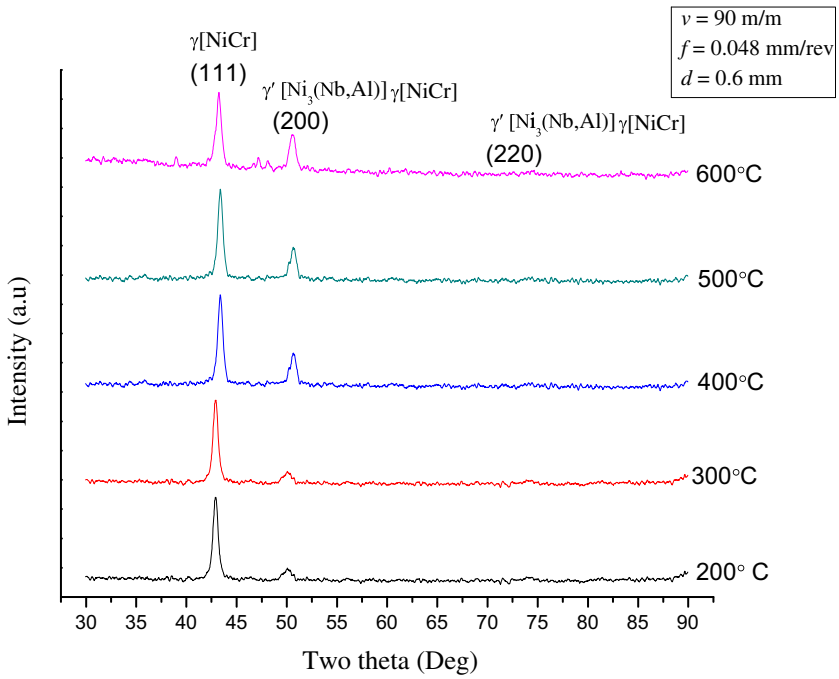

Fig. 9 XRD analysis of the phase transformation of the machined surfaces at different workpiece temperatures such as 200, 300, 400, 500 and 600 °C

this leads to smaller grain size and in turn increases the hardness on the surface and subsurface of the machined parts.

3.8 X – ray diffraction (XRD)

The machined samples were examined using X- ray diffraction (XRD). The peaks were observed at 43.06° (111), 50.79° (200) and 74.67° (220). The peaks reveal the presence of γ-Ni matrix precipitates with face-centered cubic (FCC) crystal structure. The intermetallic phases such as γ-NiCr, $\gamma'Ni_3Al$ and γ'-Ni_3Nb are precipitated in the γ-Ni matrix. By comparing the XRD peaks broadening and intensity ratio between different workpiece temperatures from 200 °C to 600 °C, a qualitative evaluation of the metallurgical changes was done as shown in Fig. 9. There are neither phase changes, nor broadening of the peaks that were observed at different machining conditions. It shows that the temperature generated in the cutting zone was not considerable enough to cause the possible phase transformation.

4 Conclusions

In this work, the effect of process parameters like cutting speed, feed rate, depth of cut and workpiece temperature in thermally assisted machining of Inconel 718 on cutting force, surface roughness, and tool wear have been investigated. The conclusions are listed based on the experimental work.

1. Process parameters with high cutting speed, low feed rate, low depth of cut and high workpiece temperature gave better surface finish and low cutting force while machining Inconel 718 with a TiAlN multilayer coated tool.
2. At high cutting speed, the type of wear observed in thermally assisted machining was abrasive, adhesive, diffusion, and microchipping.
3. The microhardness increases as the workpiece temperature increases, hence TAM improves the performance of the product.
4. The XRD results of thermally assisted machining reveal that there are neither phase changes nor broadening of the peaks that were observed at different machining conditions.

References

1. Pawade RS, Joshi SS (2011) Multi-objective optimization of surface roughness and cutting forces in high-speed turning of Inconel 718 using Taguchi grey relational analysis (TGRA). Int J Adv Manuf Technol 56:47–62
2. Ren X, Liu Z (2016) Influence of cutting parameters on work hardening behavior of surface layer during turning superalloy Inconel 718. International Journal of Advanced Manufacturing Technology, pp 1–9
3. Attia H, Tavakoli S, Vargas R, Thomson V (2010) Laser-assisted high-speed finish turning of superalloy Inconel 718 under dry conditions. CIRP Ann Manuf Technol 59:83–88
4. Liu F, Lin X, Yang G, Song M, Chen J, Huang W (2011) Microstructure and residual stress of laser rapid formed Inconel 718 nickel-base superalloy. Opt Laser Technol 43:208–213
5. Sugihara T, Takemura S, Enomoto T (2015) Study on high-speed machining of Inconel 718 focusing on tool surface topography of CBN cutting tool. International Journal of Advanced Manufacturing Technology, pp 9–17
6. García V, Arriola I, Gonzalo O, Leunda J (2013) Mechanisms involved in the improvement of Inconel 718 maChinability by laser assisted machining (LAM). Int J Mach Tools Manuf 74: 19–28
7. Bermingham MJ, Palanisamy S, Dargusch MS (2012) Understanding the tool wear mechanism during thermally assisted machining Ti-6Al-4V. Int J Mach Tools Manuf 62:76–87
8. Shokrani A, Dhokia V (2012) NewmanST Environmentally conscious machining of difficult-to-machine materials with regard to cutting fluids. Int J Mach Tools Manuf 57:83–101
9. Tebaldo V, Di Confiengo GG, Faga M. G. (2016) Sustainability in machining: 'Eco-friendly' turning of Inconel 718. Surface characterisation and economic analysis. J Clean Prod 140: 1567–1577
10. Sanchez LE, Mello HJ, Neto RR, Davim JP (2014) Hot turning of a difficult-to-machine steel (sae xev-f) aided by infrared radiation. Int J Adv Manuf Technol 73:887–898
11. Thandra SK, Choudhury SK (2010) Effect of cutting parameters on cutting force, surface finish and tool wear in hot machining. Int J Mach Mach Mater 7:260–273
12. Anderson M, Patwa R, Shin YC (2006) Laser-assisted machining of Inconel 718 with an economic analysis. Int J Mach Tools Manuf 46:1879–1891
13. Kitagawa T, Maekawa K, Kubo A (1988) Plasma hot machining for high hardness metals. Bull Japan Soc Precis Eng 22:145–151
14. Hinds BK, Almeida SM (1981) Plasma arc heating for hot machining. Int J Mach Tool Des Res 21:143–152
15. Attia H, Tavakoli S, Vargas R, Thomson V (2010) Laser-assisted high-speed finish turning of superalloy Inconel 718 under dry conditions. CIRP Ann Manuf Technol 59:83–88
16. Zhuang K, Zhang X, Zhu D, Ding H (2015) Employing preheating- and cooling-assisted technologies in machining of Inconel 718 with ceramic cutting tools: towards reducing tool wear and improving surface integrity. Int J Adv Manuf Technol 80:1815–1822
17. Sharma P, Chakradhar D, Narendranath S (2015) Evaluation of WEDM performance characteristics of Inconel 706 for turbine disk application. Mater Des 88:558–566
18. Lima JG, Ávila RF, Abrão AM, Faustino M, Davim JP (2005) Hard turning: AISI 4340 high strength low alloy steel and AISI D2 cold work tool steel. J Mater Process Technol 169:388–395
19. Suresh R, Basavarajappa S, Samuel GL (2012) Some studies on hard turning of AISI 4340 steel using multilayer coated carbide tool. Measurement 45:1872–1884
20. Sobiyi K, Sigalas I, Akdogan G, Turan Y (2015) Performance of mixed ceramics and CBN tools during hard turning of martensitic stainless steel. Int J Adv Manuf Technol 77:861–871